

PAPER



Cite this: *Polym. Chem.*, 2020, **11**, 936

## Synthesis and direct assembly of linear–dendritic copolymers via CuAAC click polymerization-induced self-assembly (CPISA)<sup>†</sup>

Min Zeng,<sup>a</sup> Xiaosong Cao,<sup>b</sup> Hui Xu,<sup>b</sup> Weiping Gan,<sup>b</sup> Bradley D. Smith,<sup>b</sup> Haifeng Gao<sup>id</sup>\*<sup>b</sup> and Jinying Yuan<sup>id</sup>\*<sup>a</sup>

A one-pot method was developed for the preparation of a linear–dendritic copolymer and its assemblies via copper-catalyzed azide–alkyne cycloaddition (CuAAC) click polymerization-induced self-assembly (CPISA). By utilizing a tris-triazoleamine-functionalized poly(ethylene glycol) (PEG) chain as a linear macroinitiator and a trifunctional AB<sub>2</sub> with one alkynyl group and two azido groups as a monomer, we successfully conducted CuAAC polymerization in methanol, water, or a methanol/water mixture with a solid content of 15 wt%. All polymerizations reached high monomer conversion and the rate of polymerization was readily tailored by the fraction of water in the solvent. The polymerization of the AB<sub>2</sub> monomer from the PEG macroinitiator produced solvent-insoluble dendritic blocks that assembled under polymerization conditions to form spherical micelles and large compound micelles, characterized by dynamic light scattering and transmission electron microscopy. This strategy broadens the topological architecture of copolymers synthesized by the PISA process and puts forward a new methodology for direct preparation of nanostructures based on linear–dendritic polymers.

Received 30th October 2019,  
Accepted 7th December 2019

DOI: 10.1039/c9py01636h

rsc.li/polymers

## Introduction

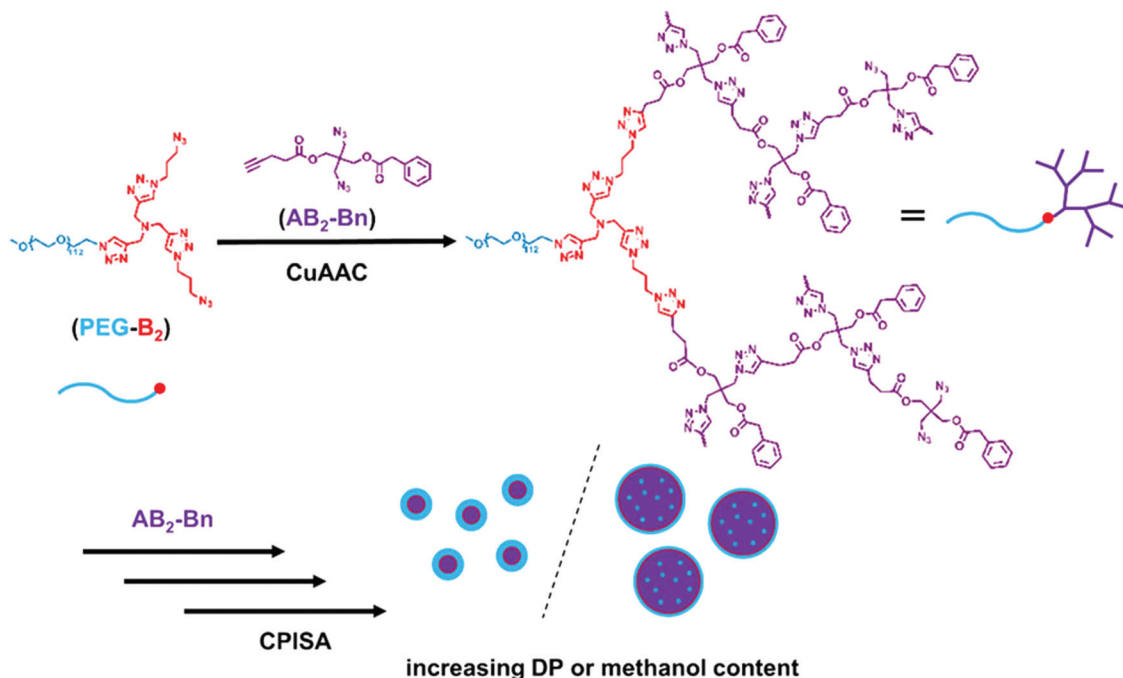
Self-assembly of block copolymers is a powerful method to prepare polymeric nanomaterials with varied morphologies and functionalities.<sup>1–6</sup> Despite advances, traditional self-assembly strategies are often conducted at low polymer concentrations (<1 wt%) and require multiple steps, limiting large-scale fabrication of materials and in-depth exploration of their applications.<sup>7,8</sup> Recently, polymerization-induced self-assembly (PISA) has emerged as an alternative one-pot technique for *in situ* preparation of polymeric nanoparticles at high solid concentrations (typically >10 wt%).<sup>9–22</sup> PISA is usually conducted under dispersion or emulsion conditions, where polymerization induces system heterogeneity and polymer assembly. In other words, a soluble polymer in an appropriate solvent becomes insoluble after chain extension by polymerization of a second monomer, resulting in the assembly of amphiphilic copolymers into nanoparticles.

To date, PISA has been predominantly performed using various types of controlled/living radical polymerization techniques, most notably, reversible addition–fragmentation chain transfer (RAFT) polymerization.<sup>22–32</sup> Due to the requirements of the PISA process and the mechanism of RAFT polymerization, most reported PISA-made nanoparticles are composed of linear block copolymers.<sup>33–37</sup> As polymer architecture is a well-known parameter for the morphology of block copolymer assemblies and has profound influence on their functions,<sup>38</sup> it is initially surprising to realize that very few studies have been published on approaching nonlinear polymer structures using the PISA technique. For example, Zhang and coworkers designed star block copolymer assemblies using 3- and 4-arm star poly(4-vinylpyridine) macromolecular chain transfer agents (macro-CTAs) via RAFT dispersion polymerization processes.<sup>39</sup> By increasing the number of arms, several interesting morphologies of the star block copolymer assemblies, including small-sized vesicles, lacunal nanospheres, and porous nanospheres, could be prepared. Similarly, Sumerlin and An *et al.* reported the synthesis of star block copolymer assemblies via RAFT dispersion polymerization by using two-CTA modified poly(ethylene glycol) as a macro-CTA.<sup>29</sup> Besides these star block copolymer structures, it is within our best knowledge that there has been no report on the synthesis and assembly of branched amphiphilic block copolymers using PISA processes.

<sup>a</sup>Key Lab of Organic Optoelectronics and Molecular Engineering of Ministry of Education, Department of Chemistry, Tsinghua University, 100084 Beijing, China. E-mail: yuanjy@mail.tsinghua.edu.cn

<sup>b</sup>Department of Chemistry and Biochemistry, University of Notre Dame, Notre Dame, Indiana 46556, USA. E-mail: hgao@nd.edu

<sup>†</sup>Electronic supplementary information (ESI) available. See DOI: 10.1039/c9py01636h



**Scheme 1** The synthetic routes to linear-dendritic copolymer assemblies *via* CuAAC click polymerization-induced self-assembly (CPISA).

Linear-dendritic copolymers are emerging as an attractive category of block copolymers in both academia and industry as the polymer by combining the linear chains and dendritic structures exhibits excellent properties, such as good encapsulation, multiple chain-end functionalities and unique self-assembly properties.<sup>40–44</sup> Self-assembly of amphiphilic linear-dendritic copolymers has become an active area in self-assembling materials. However, traditional self-assembly techniques for linear-dendritic copolymers were limited to a low solid content and require multiple steps, which largely preclude their scale-up. As a result, development of a new strategy for the self-assembly of linear-dendritic copolymers with a high solid content is still needed.

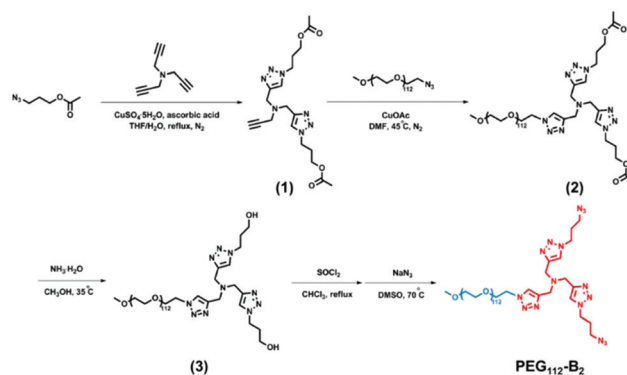
Hyperbranched (or highly branched) polymers, as an important type of dendritic polymer, have attracted great attention owing to their fascinating features including one-pot syntheses, high degree of functionalization, and arborescent structures.<sup>45–59</sup> To synthesize hyperbranched polymers with controlled structures, the Gao group has recently reported a living chain-growth polymerization of a trifunctional AB<sub>2</sub> monomer *via* a copper-catalyzed azide-alkyne cycloaddition (CuAAC) reaction.<sup>60–64</sup> This method, exhibiting both high monomer conversion and well-defined chain-growth polymerization, could potentially be applied in biphasic dispersion systems to achieve assembled structures of hyperbranched polymers. In this contribution, we for the first time developed a PISA method for CuAAC polymerization of AB<sub>2</sub> monomers to prepare linear-dendritic copolymers and their assemblies *via* CuAAC-based PISA (CPISA, Scheme 1). The AB<sub>2</sub>-Bn monomer with a benzyl pendant group and a tris-triazoleamine-functionalized poly(ethylene glycol) (PEG<sub>112</sub>-B<sub>2</sub>) macroinitiator were

synthesized. Both dispersion and emulsion CuAAC polymerizations of AB<sub>2</sub>-Bn were performed to prepare linear-dendritic copolymer assemblies in one pot.

## Results and discussion

### Synthesis of the PEG<sub>112</sub>-B<sub>2</sub> macroinitiator

To prepare the macroinitiator stabilizer block, a tris-triazoleamine-functionalized poly(ethylene glycol) (PEG<sub>112</sub>-B<sub>2</sub>) that contained two terminal azido groups (Scheme 2) was designed and synthesized. Our previous results confirm that the central tris-triazoleamine motif shows strong complexation with the Cu(I) catalyst and predominantly confines the Cu catalyst to the PEG macroinitiator even before the polymerization of the



**Scheme 2** The synthetic routes to the PEG<sub>112</sub>-B<sub>2</sub> macroinitiator.

AB<sub>2</sub> monomer.<sup>61,65</sup> The detailed synthesis and molecular characterization are provided in the ESI.† <sup>1</sup>H NMR spectroscopy and size exclusion chromatography (SEC) were used

to characterize the chemical structure and molecular weight of the PEG<sub>112</sub>-B<sub>2</sub> macroinitiator, respectively (Fig. 1). The degree of end-group functionalization of PEG<sub>112</sub> can be estimated by the area ratio of the signal at  $\delta = 2.17$  ppm (b in Fig. 1A) and the signal at  $\delta = 4.55$  ppm (f in Fig. 1A), and it is suggested that the degree of end-group functionalization is more than 97%. In SEC with DMF as the mobile phase, the PEG<sub>112</sub>-B<sub>2</sub> showed an apparent number-average molecular weight  $M_{n, RI} = 4800$  with a low polydispersity  $D = 1.04$ , based on linear poly (methyl methacrylate) PMMA standards with a refractive index (RI) detector.

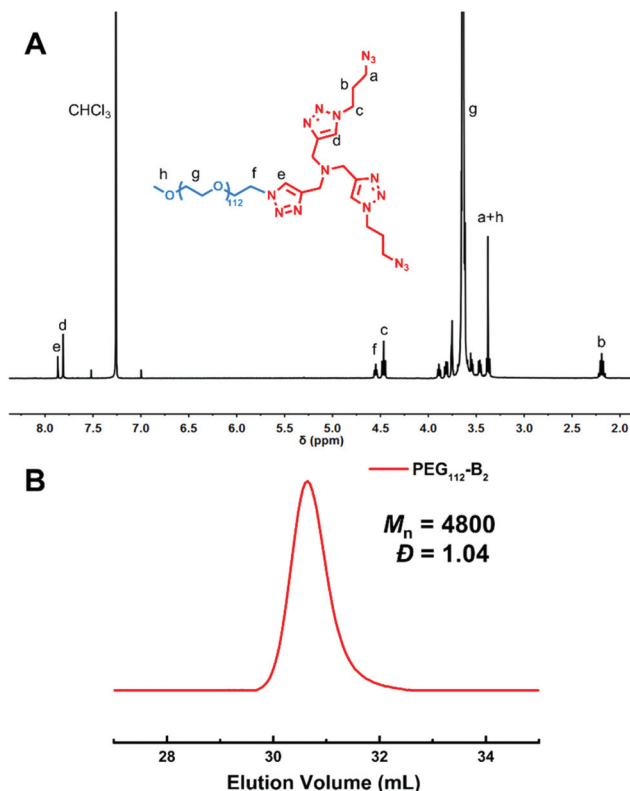


Fig. 1 (A) <sup>1</sup>H NMR spectrum of PEG<sub>112</sub>-B<sub>2</sub> with CDCl<sub>3</sub> as the solvent at 25 °C; (B) SEC trace recorded for PEG<sub>112</sub>-B<sub>2</sub>.

### Synthesis and direct assembly of PEG<sub>112</sub>-p(AB<sub>2</sub>-Bn)<sub>x</sub> via CPISA

To demonstrate the synthesis and assembly of linear-dendritic copolymers under CPISA conditions, an AB<sub>2</sub>-Bn monomer (Scheme 1, S1 and Fig. S1†) carrying a benzyl (Bn) pendant group was selected for CuAAC polymerization using the PEG<sub>112</sub>-B<sub>2</sub> as the macroinitiator, in which appropriate solvents or their mixture was critical to ensure that the second hyper-branched block was not soluble and could self-assemble into nanostructures, such as core-shell structures. As the first attempt, a CuAAC polymerization of the AB<sub>2</sub>-Bn monomer was carried out in a mixture of methanol/water (90/10, by wt) at 45 °C using a feed ratio of [AB<sub>2</sub>-Bn]<sub>0</sub>/[PEG<sub>112</sub>-B<sub>2</sub>]<sub>0</sub> = 80/1. The polymerization was conducted at 15 wt% solid content, which was much higher than that in the co-solvent method for the assembly of the preformed amphiphilic block copolymer (usually <1 wt%).<sup>9</sup> As the polymerization started, kinetic studies were performed by taking a series of aliquot samples at different times. As shown in Fig. 2A, the conversions of the AB<sub>2</sub>-Bn monomer increased with polymerization time and reached 98% within 24 h, as determined by <sup>1</sup>H NMR spec-

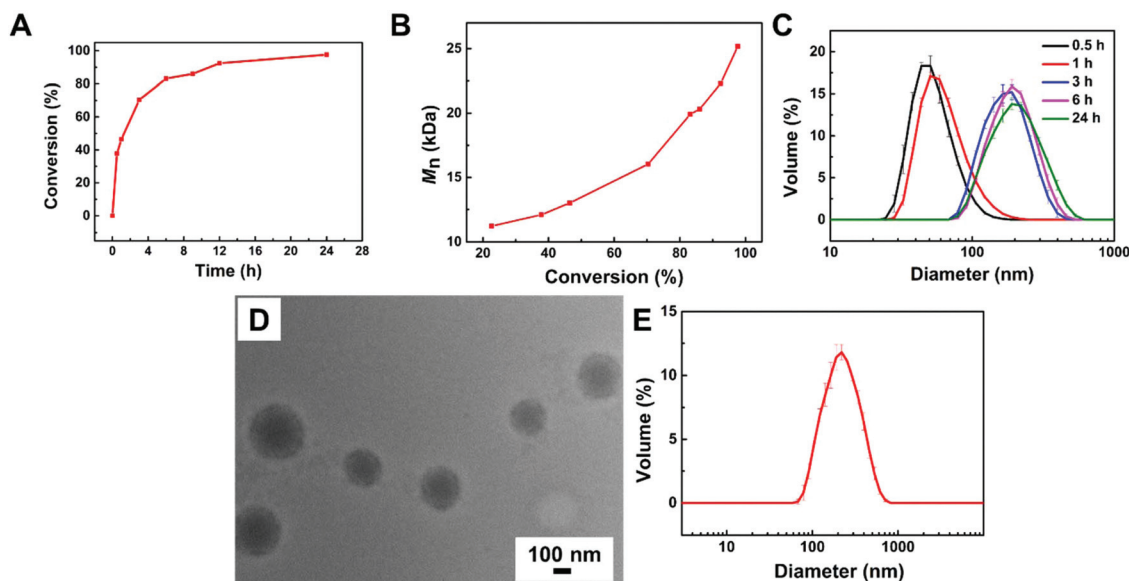


Fig. 2 (A) Conversion, (B) evolution of  $M_n$  with the monomer conversion and (C) DLS characterization of the PEG<sub>112</sub>-p(AB<sub>2</sub>-Bn)<sub>80</sub> assemblies as a function of time prepared via dispersion CuAAC polymerization in methanol/water (90/10, by wt) at 45 °C; (D) TEM image and (E) DLS characterization of the PEG<sub>112</sub>-p(AB<sub>2</sub>-Bn)<sub>80</sub> assemblies.

troscopy. SEC characterization of purified polymers showed an increased apparent molecular weight of the polymer product as a function of AB<sub>2</sub>-Bn monomer conversion (Fig. 2B). This result confirmed the polymerization of monomers and the production of linear–dendritic copolymers although a shoulder peak at a low volume direction and an oligomer peak existed in the SEC curves, probably due to the undesired monomer–monomer reaction in parallel to the desired monomer polymerization from the macroinitiator (Fig. S2†). Meanwhile, the progress of polymerization changed the reaction system from a transparent solution to a translucent dispersion after 0.5 h, indicating the generation of assembled nanostructures whose hydrodynamic diameters increased and finally reached 215 nm after 24 h (Fig. 2C) when the polymerization was completed.

After polymerization, a portion of the polymer product was purified to characterize the polymer structures and molecular weights by <sup>1</sup>H NMR and SEC, while another portion of the samples was prepared for the characterization of polymer assemblies using transmission electron microscopy (TEM) and

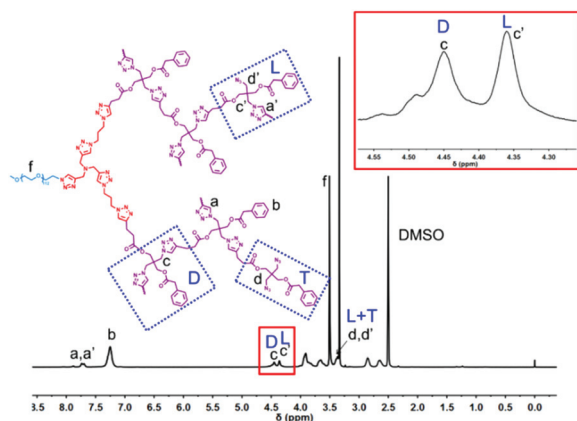


Fig. 3 <sup>1</sup>H NMR spectrum of PEG<sub>112</sub>-p(AB<sub>2</sub>-Bn)<sub>80</sub> with DMSO-d<sub>6</sub> as the solvent at 25 °C.

dynamic light scattering (DLS). The <sup>1</sup>H NMR spectrum of purified polymer PEG<sub>112</sub>-p(AB<sub>2</sub>-Bn)<sub>80</sub> (Fig. 3) indicates resolved peaks from both PEG<sub>112</sub> and p(AB<sub>2</sub>-Bn)<sub>80</sub> blocks. By comparing the methylene proton peak (f in Fig. 3) from the PEG<sub>112</sub> block and the phenyl proton peak (b in Fig. 3) from the p(AB<sub>2</sub>-Bn)<sub>80</sub> block, the integral area ratio of peaks b and f was consistent with the feed ratio of [AB<sub>2</sub>-Bn]<sub>0</sub>/[PEG<sub>112</sub>-B<sub>2</sub>]<sub>0</sub> and high monomer conversion. This result further confirmed the successful synthesis of linear–dendritic copolymer PEG<sub>112</sub>-p(AB<sub>2</sub>-Bn)<sub>80</sub> and the high monomer conversion of the CPISA strategy. The degree of branching (DB) of purified polymer PEG<sub>112</sub>-p(AB<sub>2</sub>-Bn)<sub>80</sub> was determined by <sup>1</sup>H NMR spectroscopy by following the published method.<sup>64,66</sup> The calculated result based on equation  $DB = 2D/(2D + L)$  was about DB = 0.53, in which *D* and *L* represent the molar fraction of the dendritic unit and linear unit in the hyperbranched polymer quantified by integrating the peaks *c* and *c'*. It is worth noting that this DB value was lower than that of hyperbranched polymers synthesized in solution CuAAC polymerization (*e.g.*, DB > 0.80)<sup>64</sup> primarily because of the partition of Cu(i) catalysts between the organic polymer phase and the continuous methanol/water phase. Due to the charged nature of the Cu(i) catalyst, its escape from the polymerizing particle into the methanol/water phase decreased the effective concentration and residing time of the Cu catalyst on the *L* unit in the polymer, resulting in a slower reaction of the dangling azido group to convert the *L* unit to *D* unit and a lower DB value of the polymer.

Meanwhile, characterization of the polymers by SEC coupled with a multi-angle laser light scattering (MALLS) detector and RI detector determined the absolute number-average molecular weights  $M_{n, \text{MALLS}} = 70\,900$  and the  $M_{n, \text{RI}} = 24\,500$  (Table 1, entry 8). The higher value of  $M_{n, \text{MALLS}}$  than  $M_{n, \text{RI}}$  indicates a compact molecular structure of the linear–dendritic copolymer.

In addition to determining the molecular characteristics, the assembled nanostructures in dispersion were characterized by both TEM and DLS. Fig. 2D suggests that spherical micelles

Table 1 Summary of the linear–dendritic copolymers PEG<sub>112</sub>-p(AB<sub>2</sub>-Bn)<sub>x</sub> and their assemblies

| Entry | Solvent CH <sub>3</sub> OH/H <sub>2</sub> O by wt | Feed ([PEG <sub>112</sub> -B <sub>2</sub> ] <sub>0</sub> /[AB <sub>2</sub> -Bn] <sub>0</sub> ) | Conv. <sup>a</sup> (%) | $M_{n, \text{MALLS}}$ <sup>b</sup> | DB <sup>c</sup> | $M_{n, \text{RI}}$ <sup>d</sup> | $\mathcal{D}$ <sup>d</sup> | DLS                     |                  |
|-------|---|--|------------------------|------------------------------------|-----------------|---------------------------------|----------------------------|-------------------------|------------------|
|       |   |  |                        |                                    |                 |                                 |                            | $D_h$ <sup>e</sup> (nm) | PdI <sup>e</sup> |
| 1     | 100/0   | 1/20   | 96                     | 18 400                             | 0.47            | 13 000                          | 1.19                       | 23                      | 0.092            |
| 2     | 100/0   | 1/40   | 98                     | 41 600                             | 0.52            | 22 100                          | 1.07                       | 84                      | 0.260            |
| 3     | 100/0   | 1/80   | 96                     | 73 700                             | 0.53            | 31 000                          | 1.19                       | 1031                    | 0.290            |
| 4     | 100/0   | 1/120  | 97                     | 95 400                             | 0.52            | 36 300                          | 1.34                       | 1368                    | 0.460            |
| 5     | 95/5  | 1/80   | 99                     | 82 500                             | 0.52            | 25 200                          | 1.63                       | 1093                    | 0.309            |
| 6     | 90/10   | 1/20   | 99                     | 29 700                             | 0.52            | 16 200                          | 1.28                       | 34                      | 0.083            |
| 7     | 90/10   | 1/40   | 99                     | 34 500                             | 0.53            | 19 700                          | 1.31                       | 91                      | 0.302            |
| 8     | 90/10   | 1/80   | 98                     | 70 900                             | 0.53            | 24 500                          | 1.45                       | 237                     | 0.136            |
| 9     | 90/10   | 1/120  | 98                     | 113 200                            | 0.52            | 40 600                          | 1.40                       | 320                     | 0.099            |
| 10    | 0/100   | 1/80   | 93                     | 67 900                             | 0.51            | 33 400                          | 1.68                       | 34                      | 0.286            |

<sup>a</sup> Monomer AB<sub>2</sub>-Bn conversion determined by <sup>1</sup>H NMR spectroscopy. <sup>b</sup> Absolute number-average molecular weight ( $M_{n, \text{MALLS}}$ ) determined by DMF SEC with a MALLS detector. <sup>c</sup> Degree of branching (DB) determined by <sup>1</sup>H NMR spectroscopy. <sup>d</sup> Apparent number-average molecular weight ( $M_{n, \text{RI}}$ ) and molecular weight distribution ( $\mathcal{D} = M_w/M_n$ ) determined by DMF SEC with a RI detector based on linear PMMA standards. <sup>e</sup> Hydrodynamic diameter ( $D_h$ ) and polydispersity index (PdI) determined by DLS analysis of the assembly samples in the corresponding reaction solvent after dialysis.

were obtained from the PEG<sub>112</sub>-p(AB<sub>2</sub>-Bn)<sub>80</sub> assemblies, and the DLS result in Fig. 2E shows that the hydrodynamic diameter ( $D_h$ ) of these assemblies was  $D_h = 237$  nm with a narrow size distribution of 0.136. These results suggested the successful CPISA process to form well-defined micellar structures by using a mixed solvent of methanol/water *via* dispersion CuAAC polymerization of the AB<sub>2</sub>-Bn monomer.

Based on the initial success as discussed above, several other linear-dendritic copolymer assemblies with varied DPs of the hyperbranched segment, *i.e.*, PEG<sub>112</sub>-p(AB<sub>2</sub>-Bn)<sub>x</sub> with  $x = 20, 40, 120$ , were produced using similar procedures, in order to explore morphological evolution of the assemblies as a function of molecular weights of dendritic segment. Each polymerization was carried out in methanol/water (90/10, by wt) with a solid content of 15 wt%. In all these polymerizations, high monomer conversion ( $\geq 98\%$ ) was achieved before the polymerizations were stopped. It was found that the hydrodynamic diameter of these linear-dendritic copolymer assemblies increased from  $D_h = 34$  to 320 nm as the feed ratio of the AB<sub>2</sub>-Bn monomer to PEG macroinitiator increased from  $x = 20$  to 120 (Fig. 4D). TEM results indicated spherical micelles for all three PEG<sub>112</sub>-p(AB<sub>2</sub>-Bn)<sub>x</sub> ( $x = 20, 40, 120$ ) linear-dendritic copolymer assemblies (Fig. 4A–C). As the length of the PEG stabilizer block has great influence on the final morphologies, the long PEG<sub>112</sub> block led to effective steric stabilization of the hydrophobic dendritic block and prevented evolution in copolymer morphology,<sup>67–69</sup> so that the variation of  $x$  between 20 and 120 resulted in the spherical morphology of the assembled nanostructures.

Besides altering the size of the dendritic block, we further evaluated the influence of solvents on the structures of linear-dendritic copolymers and their assembly morphology, since a solvent is an important factor in the CPISA process. For comparison, several CuAAC polymerizations of AB<sub>2</sub>-Bn with a

target composition of PEG<sub>112</sub>-p(AB<sub>2</sub>-Bn)<sub>80</sub> were performed in methanol (100/0), methanol/water (95/5, by wt), and water (0/100), respectively (Table 1). All polymerizations carried out at 45 °C reached high monomer conversions although the polymerization rate increased with the content of water in the solvent. For instance, the CPISA in pure water observed the fastest polymerization and reached 93% monomer conversion in 5 h (Fig. 5A). As the AB<sub>2</sub>-Bn monomer is insoluble in water, the CPISA system formed emulsion before polymerization. The PEG macroinitiator assisted the emulsification of monomers into discrete micelles and droplets, which facilitated faster polymerization due to neat monomer concentration inside and the compartmentalization effect.<sup>70</sup> Regarding the molecular weight evolution, all polymerizations showed increased polymer molecular weights *i.e.*,  $M_{n, RI}$ , with conversion as shown in Fig. 5B. Meanwhile, the molecular weight of the polymer from CPISA in pure methanol (100/0) was larger than that from the mixed solvent methanol/water (95/5, by wt), probably due to the different extent of monomer-monomer reactions in these systems. As competing with the monomer-polymer reaction, the monomer-monomer reaction formed oligomers and decreased the overall molecular weight of the linear-dendritic copolymer.

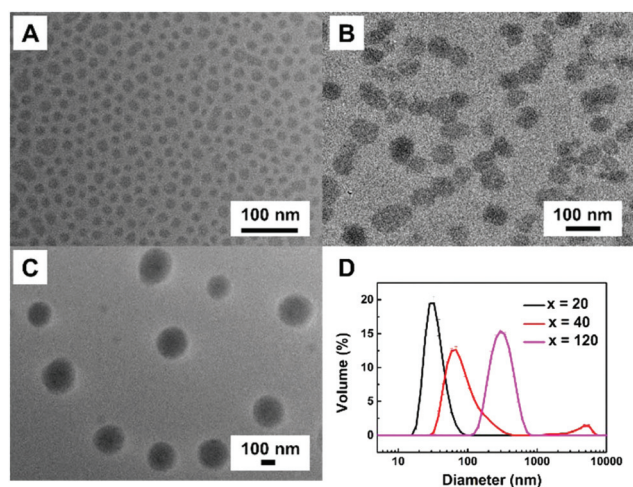


Fig. 4 TEM images of (A) PEG<sub>112</sub>-p(AB<sub>2</sub>-Bn)<sub>20</sub>, (B) PEG<sub>112</sub>-p(AB<sub>2</sub>-Bn)<sub>40</sub> and (C) PEG<sub>112</sub>-p(AB<sub>2</sub>-Bn)<sub>120</sub> assemblies, and (D) DLS characterization of PEG<sub>112</sub>-p(AB<sub>2</sub>-Bn)<sub>x</sub> ( $x = 20, 40, 120$ ) assemblies prepared *via* dispersion CuAAC polymerization in methanol/water (90/10, by wt) at 45 °C.

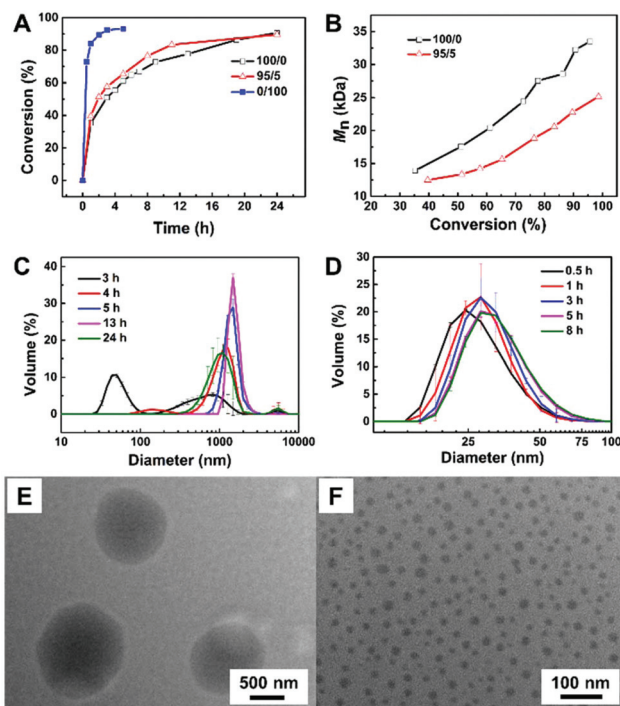


Fig. 5 (A) Evolution of monomer conversions with time in the preparation of PEG<sub>112</sub>-p(AB<sub>2</sub>-Bn)<sub>80</sub> by CuAAC polymerization in methanol (100/0), methanol/water (95/5, by wt), and water (0/100); (B) evolution of  $M_{n, RI}$  with monomer conversion in preparation of PEG<sub>112</sub>-p(AB<sub>2</sub>-Bn)<sub>80</sub> by CuAAC polymerization in methanol (100/0) and methanol/water (95/5, by wt); (C) DLS characterization of the PEG<sub>112</sub>-p(AB<sub>2</sub>-Bn)<sub>80</sub> assemblies as a function of time prepared *via* CPISA in (C) methanol (100/0) and (D) water (0/100); TEM images of the final PEG<sub>112</sub>-p(AB<sub>2</sub>-Bn)<sub>80</sub> assemblies prepared *via* CPISA in (E) methanol (100/0) and (F) water (0/100).

Interestingly, DLS characterization studies of the PEG<sub>112</sub>-p(AB<sub>2</sub>-Bn)<sub>80</sub> assemblies prepared *via* CPISA in methanol and water were significantly different. For the polymerization in methanol, the  $D_h$  of the assemblies increased from  $D_h = 52$  to 1416 nm, and eventually stabilized at 1031 nm (Fig. 5C). The degree of solvation of methanol and AB<sub>2</sub>-Bn monomer to the assemblies decreased as the polymerization proceeded, which resulted in a slight decrease of the size of assemblies after polymerization for 24 h.<sup>70,71</sup> The TEM image in Fig. 5E reveals their morphology to be large compound micelles as the dimension of assemblies was much larger than the extended contour length of the linear dendritic polymer. This result was in agreement with the observed large  $D_h$  size of the PEG<sub>112</sub>-p(AB<sub>2</sub>-Bn)<sub>80</sub> assemblies in methanol, indicating an entangled PEG chain embedded inside the compound micelles.<sup>72</sup> Similarly, large compound micelles were also obtained in PEG<sub>112</sub>-p(AB<sub>2</sub>-Bn)<sub>80</sub> assemblies prepared in methanol/water (95/5, by wt) (Fig. S3†). For the CPISA in water, the hydrodynamic size of assemblies varied in a narrow range from  $D_h$  28 to 33 nm (Fig. 5D) as the CuAAC polymerization of the water-insoluble AB<sub>2</sub>-Bn monomer in water was an emulsion instead of a dispersion. TEM confirms that spherical micelles were obtained for the PEG<sub>112</sub>-p(AB<sub>2</sub>-Bn)<sub>80</sub> assemblies synthesized in water (Fig. 5F).

Since the CPISA in pure methanol reassembled a true dispersion polymerization system and produced large compound micelles as a product, further studies were carried out to prepare a series of PEG<sub>112</sub>-p(AB<sub>2</sub>-Bn)<sub>x</sub> ( $x = 20, 40, 80, 120$ ) linear-dendritic copolymer assemblies in methanol (Table 1). Along with PEG<sub>112</sub>-p(AB<sub>2</sub>-Bn)<sub>80</sub> assemblies, the  $D_h$  of these four assemblies increased from 23 to 1368 nm and the morphology transformed from spherical micelles to large compound micelles with the increase of the DP of the solvophobic blocks (Fig. 6A–D). When considering both series of PEG<sub>112</sub>-p(AB<sub>2</sub>-

Bn)<sub>x</sub> assemblies with varied  $x$  values and different solvents as methanol/water (90/10, by wt) or pure methanol, it was confirmed that both the molecular size of the dendritic block and polymerization solvent were vital to the morphologies of assembled nanostructures in these CPISA systems.

## Conclusions

In summary, we successfully developed a method to fabricate a linear-dendritic copolymer and its assemblies *via* CuAAC polymerization using the PISA formula. This strategy, termed CPISA, was performed in various solvents, including methanol, methanol/water mixture and water, to target different DPs of the dendritic block in high conversions. Both experimental variables, the solvent and the DP, exhibited a significant effect on the polymerization kinetics and the morphology of the assemblies. A higher water content not only increased the polymerization rate, but also produced micelle-like linear-dendritic copolymer assemblies. Meanwhile, pure methanol as a solvent and a higher target DP produced large compound micelles as the CPISA in water started as an emulsion while the CPISA in methanol started as a solution before the polymerization-induced assembly progressed with monomer conversion. These results demonstrate for the first time the preparation of linear-dendritic copolymer assemblies *via* the CPISA process and provide a useful approach to fabricate nanostructured assemblies based on dendritic polymers for potential applications.

## Conflicts of interest

There are no conflicts to declare.

## Acknowledgements

The National Natural Science Foundation of China (Project No. 51573086 and 21871162) is acknowledged for financial support. M. Z. thanks the Tsinghua Scholarship for Overseas Graduates Studies. H. G. thanks the National Science Foundation (CHE-1554519) for financial support. M. Z., B. D. S. and H. G. thank Asia Research Collaboration Grant, Notre Dame International for partial support of this research.

## References

- 1 Y. Mai and A. Eisenberg, *Chem. Soc. Rev.*, 2012, **41**, 5969–5985.
- 2 U. Tritschler, S. Pearce, J. Gwyther, G. R. Whittell and I. Manners, *Macromolecules*, 2017, **50**, 3439–3463.
- 3 A. Blanazs, S. P. Armes and A. J. Ryan, *Macromol. Rapid Commun.*, 2009, **30**, 267–277.
- 4 A. Rösler, G. W. M. Vandermeulen and H.-A. Klok, *Adv. Drug Delivery Rev.*, 2012, **64**, 270–279.

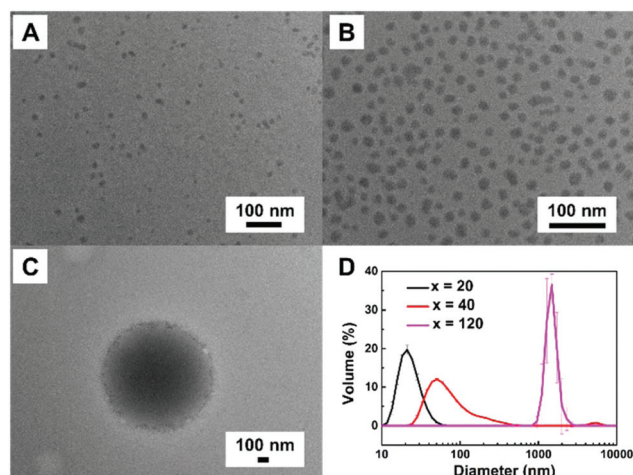


Fig. 6 TEM images of (A) PEG<sub>112</sub>-p(AB<sub>2</sub>-Bn)<sub>20</sub>, (B) PEG<sub>112</sub>-p(AB<sub>2</sub>-Bn)<sub>40</sub>, and (C) PEG<sub>112</sub>-p(AB<sub>2</sub>-Bn)<sub>120</sub> assemblies, and (D) DLS characterization of PEG<sub>112</sub>-p(AB<sub>2</sub>-Bn)<sub>x</sub> ( $x = 20, 40, 120$ ) assemblies prepared *via* CPISA in methanol.

- 5 R. C. Hayward and D. J. Pochan, *Macromolecules*, 2010, **43**, 3577–3584.
- 6 J. K. Kim, S. Y. Yang, Y. Lee and Y. Kim, *Prog. Polym. Sci.*, 2010, **35**, 1325–1349.
- 7 N. S. Cameron, M. K. Corbierre and A. Eisenberg, *Can. J. Chem.*, 1999, **77**, 1311–1326.
- 8 Y. Wang, M. Huo, M. Zeng, L. Liu, Q.-Q. Ye, X. Chen, D. Li, L. Peng and J.-Y. Yuan, *Chin. J. Polym. Sci.*, 2018, **36**, 1321–1327.
- 9 S. L. Canning, G. N. Smith and S. P. Armes, *Macromolecules*, 2016, **49**, 1985–2001.
- 10 B. Charleux, G. Delaittre, J. Rieger and F. D'Agosto, *Macromolecules*, 2012, **45**, 6753–6765.
- 11 W.-M. Wan, X.-L. Sun and C.-Y. Pan, *Macromolecules*, 2009, **42**, 4950–4952.
- 12 S.-L. Chen, P.-F. Shi and W.-Q. Zhang, *Chin. J. Polym. Sci.*, 2017, **35**, 455–479.
- 13 M. Huo, G. Song, J. Zhang, Y. Wei and J. Yuan, *ACS Macro Lett.*, 2018, **7**, 956–961.
- 14 X.-L. Sun, D.-M. Liu, P. Wang, J.-L. Tan, K.-K. Li, L. Deng and W.-M. Wan, *Chem. Commun.*, 2017, **53**, 5005–5008.
- 15 S. Guan, Z. Deng, T. Huang, W. Wen, Y. Zhao and A. Chen, *ACS Macro Lett.*, 2019, **8**, 460–465.
- 16 J. C. Foster, S. Varlas, B. Couturaud, J. R. Jones, R. Keogh, R. T. Mathers and R. K. O'Reilly, *Angew. Chem., Int. Ed.*, 2018, **57**, 15733–15737.
- 17 J. C. Foster, S. Varlas, L. D. Blackman, L. A. Arkinstall and R. K. O'Reilly, *Angew. Chem., Int. Ed.*, 2018, **57**, 10672–10676.
- 18 X. Wang and Z. An, *Macromol. Rapid Commun.*, 2019, **40**, 1800325.
- 19 J. Tan, X. Dai, Y. Zhang, L. Yu, H. Sun and L. Zhang, *ACS Macro Lett.*, 2019, **8**, 205–212.
- 20 X.-F. Xu, C.-Y. Pan, W.-J. Zhang and C.-Y. Hong, *Macromolecules*, 2019, **52**, 1965–1975.
- 21 S. Varlas, L. D. Blackman, H. E. Findlay, E. Reading, P. J. Booth, M. I. Gibson and R. K. O'Reilly, *Macromolecules*, 2018, **51**, 6190–6201.
- 22 C. A. Figg, R. N. Carmean, K. C. Bentz, S. Mukherjee, D. A. Savin and B. S. Sumerlin, *Macromolecules*, 2017, **50**, 935–943.
- 23 J. Rieger, *Macromol. Rapid Commun.*, 2015, **36**, 1458–1471.
- 24 X. Chen, L. Liu, M. Huo, M. Zeng, L. Peng, A. Feng, X. Wang and J. Yuan, *Angew. Chem., Int. Ed.*, 2017, **56**, 16541–16545.
- 25 M. Zeng, M. Huo, Y. Feng and J. Yuan, *Macromol. Rapid Commun.*, 2018, **39**, 1800291.
- 26 J.-T. Sun, C.-Y. Hong and C.-Y. Pan, *Polym. Chem.*, 2013, **4**, 873–881.
- 27 Q. Ye, M. Huo, M. Zeng, L. Liu, L. Peng, X. Wang and J. Yuan, *Macromolecules*, 2018, **51**, 3308–3314.
- 28 M. A. Touve, C. A. Figg, D. B. Wright, C. Park, J. Cantlon, B. S. Sumerlin and N. C. Gianneschi, *ACS Cent. Sci.*, 2018, **4**, 543–547.
- 29 X. Wang, C. A. Figg, X. Lv, Y. Yang, B. S. Sumerlin and Z. An, *ACS Macro Lett.*, 2017, **6**, 337–342.
- 30 S. Qu, R. Liu, W. Duan and W. Zhang, *Macromolecules*, 2019, **52**, 5168–5176.
- 31 M. Chen, J.-W. Li, W.-J. Zhang, C.-Y. Hong and C.-Y. Pan, *Macromolecules*, 2019, **52**, 1140–1149.
- 32 C. A. Figg, A. Simula, K. A. Gebre, B. S. Tucker, D. M. Haddleton and B. S. Sumerlin, *Chem. Sci.*, 2015, **6**, 1230–1236.
- 33 W. Cai, W. Wan, C. Hong, C. Huang and C. Pan, *Soft Matter*, 2010, **6**, 5554–5561.
- 34 M. Huo, Y. Zhang, M. Zeng, L. Liu, Y. Wei and J. Yuan, *Macromolecules*, 2017, **50**, 8192–8201.
- 35 J. Tan, Q. Xu, Y. Zhang, C. Huang, X. Li, J. He and L. Zhang, *Macromolecules*, 2018, **51**, 7396–7406.
- 36 A. A. Cockram, T. J. Neal, M. J. Derry, O. O. Mykhaylyk, N. S. J. Williams, M. W. Murray, S. N. Emmett and S. P. Armes, *Macromolecules*, 2017, **50**, 796–802.
- 37 Q.-Q. Ye, M.-X. Zheng, X. Chen, D. Li, W.-G. Tian, J. Zhang and J.-Y. Yuan, *Acta Polym. Sin.*, 2019, **50**, 344–351.
- 38 J. Lesage de la Haye, X. Zhang, I. Chaduc, F. Brunel, M. Lansalot and F. D'Agosto, *Angew. Chem., Int. Ed.*, 2016, **55**, 3739–3743.
- 39 Y. Zhang, M. Cao, G. Han, T. Guo, T. Ying and W. Zhang, *Macromolecules*, 2018, **51**, 5440–5449.
- 40 I. Gitsov and J. M. J. Frechet, *Macromolecules*, 1993, **26**, 6536–6546.
- 41 F. Wurm and H. Frey, *Prog. Polym. Sci.*, 2011, **36**, 1–52.
- 42 X. Liu and I. Gitsov, *Macromolecules*, 2019, **52**, 5563–5573.
- 43 J. del Barrio, L. Oriol, C. Sánchez, J. L. Serrano, A. Di Cicco, P. Keller and M.-H. Li, *J. Am. Chem. Soc.*, 2010, **132**, 3762–3769.
- 44 D. Huang, Y. Wang, F. Yang, H. Shen, Z. Weng and D. Wu, *Polym. Chem.*, 2017, **8**, 6675–6687.
- 45 Y. Zhou, W. Huang, J. Liu, X. Zhu and D. Yan, *Adv. Mater.*, 2010, **22**, 4567–4590.
- 46 C. Zhang, Y. Fan, Y. Zhang, C. Yu, H. Li, Y. Chen, I. W. Hamley and S. Jiang, *Macromolecules*, 2017, **50**, 1657–1665.
- 47 Y. Zheng, S. Li, Z. Weng and C. Gao, *Chem. Soc. Rev.*, 2015, **44**, 4091–4130.
- 48 R. Dong, Y. Zhou and X. Zhu, *Acc. Chem. Res.*, 2014, **47**, 2006–2016.
- 49 J. A. Alfurhood, H. Sun, P. R. Bachler and B. S. Sumerlin, *Polym. Chem.*, 2016, **7**, 2099–2104.
- 50 H. Han and N. V. Tsarevsky, *Chem. Sci.*, 2014, **5**, 4599–4609.
- 51 B. Yao, T. Hu, H. Zhang, J. Li, J. Z. Sun, A. Qin and B. Z. Tang, *Macromolecules*, 2015, **48**, 7782–7791.
- 52 E. Mohammadifar, A. Bodaghi, A. Dadkhahtehrani, A. Nemati Kharat, M. Adeli and R. Haag, *ACS Macro Lett.*, 2017, **6**, 35–40.
- 53 I. N. Kurniasih, J. Keilitz and R. Haag, *Chem. Soc. Rev.*, 2015, **44**, 4145–4164.
- 54 C. Liu, Y.-Y. Fei, H.-L. Zhang, C.-Y. Pan and C.-Y. Hong, *Macromolecules*, 2019, **52**, 176–184.
- 55 M. Scharfenberg, J. Seiwert, M. Scherger, J. Preis, M. Susewind and H. Frey, *Macromolecules*, 2017, **50**, 6577–6585.

- 56 F. Li, M. Cao, Y. Feng, R. Liang, X. Fu and M. Zhong, *J. Am. Chem. Soc.*, 2019, **141**, 794–799.
- 57 Q. Wei, X. Zan, Q. Xianping, G. Öktem, K. Sahre, A. Kiriy and B. Voit, *Macromol. Chem. Phys.*, 2016, **217**, 1977–1984.
- 58 X.-X. Deng, F.-S. Du and Z.-C. Li, *ACS Macro Lett.*, 2014, **3**, 667–670.
- 59 X.-X. Deng, Y. Cui, F.-S. Du and Z.-C. Li, *Polym. Chem.*, 2014, **5**, 3316–3320.
- 60 Y. Shi, R. W. Graff, X. Cao, X. Wang and H. Gao, *Angew. Chem., Int. Ed.*, 2015, **54**, 7631–7635.
- 61 X. Cao, Y. Shi, X. Wang, R. W. Graff and H. Gao, *Macromolecules*, 2016, **49**, 760–766.
- 62 X. Cao, Y. Shi, W. Gan, H. Naguib, X. Wang, R. W. Graff and H. Gao, *Macromolecules*, 2016, **49**, 5342–5349.
- 63 Y. Shi, X. Cao, D. Hu and H. Gao, *Angew. Chem., Int. Ed.*, 2018, **57**, 516–520.
- 64 Y. Shi, X. Cao, S. Luo, X. Wang, R. W. Graff, D. Hu, R. Guo and H. Gao, *Macromolecules*, 2016, **49**, 4416–4422.
- 65 W. Gan, X. Cao, Y. Shi and H. Gao, *J. Polym. Sci., Part A: Polym. Chem.*, 2019, DOI: 10.1002/pola.29440.
- 66 D. Hölter, A. Burgath and H. Frey, *Acta Polym.*, 1997, **48**, 30–35.
- 67 E. R. Jones, M. Semsarilar, A. Blanazs and S. P. Armes, *Macromolecules*, 2012, **45**, 5091–5098.
- 68 L. A. Fielding, M. J. Derry, V. Ladmiraal, J. Rosselgong, A. M. Rodrigues, L. P. D. Ratcliffe, S. Sugihara and S. P. Armes, *Chem. Sci.*, 2013, **4**, 2081–2087.
- 69 D. Li, M. Huo, L. Liu, M. Zeng, X. Chen, X. Wang and J. Yuan, *Macromol. Rapid Commun.*, 2019, **40**, 1900202.
- 70 E. R. Jones, M. Semsarilar, P. Wyman, M. Boerakker and S. P. Armes, *Polym. Chem.*, 2016, **7**, 851–859.
- 71 F. Brunel, J. Lesage de la Haye, M. Lansalot and F. D'Agosto, *J. Phys. Chem. B*, 2019, **123**, 6609–6617.
- 72 H. Hong, Y. Mai, Y. Zhou, D. Yan and J. Cui, *Macromol. Rapid Commun.*, 2007, **28**, 591–596.